Simultaneous detection of multiple green fluorescent proteins in live cells by fluorescence lifetime imaging microscopy

Rainer Pepperkok*†, Anthony Squire‡, Stephan Geley§ and Philippe I.H. Bastiaens‡

The green fluorescent protein (GFP) has proven to be an excellent fluorescent marker for protein expression and localisation in living cells [1–5]. Several mutant GFPs with distinct fluorescence excitation and emission spectra have been engineered for intended use in multi-labelling experiments [6–9]. Discrimination of these co-expressed GFP variants by wavelength is hampered, however, by a high degree of spectral overlap, low quantum efficiencies and extinction coefficients [10], or rapid photobleaching [6]. Using fluorescence lifetime imaging microscopy (FLIM) [11–16], four GFP variants were shown to have distinguishable fluorescence lifetimes. Among these was a new variant (YFP5) with spectral characteristics reminiscent of yellow fluorescent protein [8] and a comparatively long fluorescence lifetime. The fluorescence intensities of co-expressed spectrally similar GFP variants (either alone or as fusion proteins) were separated using lifetime images obtained with FLIM at a single excitation wavelength and using a single broad band emission filter. Fluorescence lifetime imaging opens up an additional spectroscopic dimension to wavelength through which novel GFP variants can be selected to extend the number of protein processes that can be imaged simultaneously in cells.

Addresses: *Light Microscopy Unit and ‡Cell Biophysics Laboratory, Imperial Cancer Research Fund, 44 Lincoln's Inn Fields, London WC2A 3PX, UK. §Cell Cycle Control Laboratory, Clare Hall, Imperial Cancer Research Fund, Blanche Lane, South Mimms EN6 3LD, UK.

Present address: †European Molecular Biology Laboratories, Heidelberg, ALMF/Cell Biophysics Programme, 69117 Heidelberg, Germany.

Correspondence: Philippe I.H. Bastiaens
E-mail: p.bastiaens@icrf.icnet.uk

Received: 16 November 1998
Revised: 21 December 1998
Accepted: 26 January 1999

Published: 1 March 1999

Current Biology 1999, 9:269–272
http://biomednet.com/elecref/0960982200900269

Results and discussion

Frequency domain FLIM [16] was used to measure the average fluorescence lifetimes of six GFP variants, which were found to range in value from 1.3 to 3.7 ns (Table 1). Except for cyan fluorescent protein (CFP), each of the GFPs showed a similarity between their phase (τ_ϕ) and modulation (τ_M) lifetimes (Figure 1a), indicating a high degree of homogeneity in the fluorescent species [14]. Four of the six mutants — CFP, S65T, YFP10c and YFP5 — exhibited separate and distinct lifetime distributions (Table 1 and Figure 1a). The new variant YFP5, in particular, showed a well-separated and significantly longer lifetime than the others, making it an ideal partner in multi-labelling FLIM experiments. In contrast to the intensity images, the fluorescence lifetime images of all the variants displayed a mostly uniform distribution throughout the entire cell (for example, see Figure 1b,c).

Table 1

Phase and modulation lifetimes of mutant GFP variants measured by FLIM in live cells at 37°C.

GFP variant	Lifetime (ns)		Number of measurements
	τ_ϕ	τ_M	
CFP* (458 nm)	2.07 ± 0.09	2.68 ± 0.07	3
CFP* (488 nm)	1.32 ± 0.03	2.23 ± 0.05	3
S65T†	2.57 ± 0.07	2.59 ± 0.04	9
EGFP‡	2.36 ± 0.06	2.42 ± 0.03	5
GFP5§	2.42 ± 0.08	2.68 ± 0.04	7
YFP10c#	2.85 ± 0.12	2.88 ± 0.05	3
YFP5**	3.69 ± 0.15	3.60 ± 0.06	3

*[22]. †[7]. ‡Clontech. §[21]. #[22]. **See Supplementary material.

As expected, the fluorescence lifetimes were dependent on temperature, such that a decrease of approximately 400 ps was measured between room temperature (22°C) and 37°C for the mutant S65T. The pH dependence of the fluorescence lifetimes was also examined for three of the mutant GFPs. As previously observed for S65T [17], only minor changes in the lifetimes (< 200 ps) were observed over pH values exceeding the physiological range expected in live cells (see Supplementary material published with this article on the internet). This is in sharp contrast to the steady state fluorescence intensity, which drastically decreased at pH values lower than 7.0 (data not shown; [17,18]) and thus demonstrates the suitability of FLIM for the discrimination of GFP mutants even in cellular compartments subjected to significant pH changes. Indeed, a small but discernible effect of pH on the lifetime was observed in live cells for the Golgi-resident fusion protein NA–GFP5 (Table 2) — an increment of < 200 ps was found upon its relocation from the acidic environment of the Golgi to the neutral lumen of the endoplasmic reticulum (ER) [18] by addition of the fungal metabolite

Figure 1

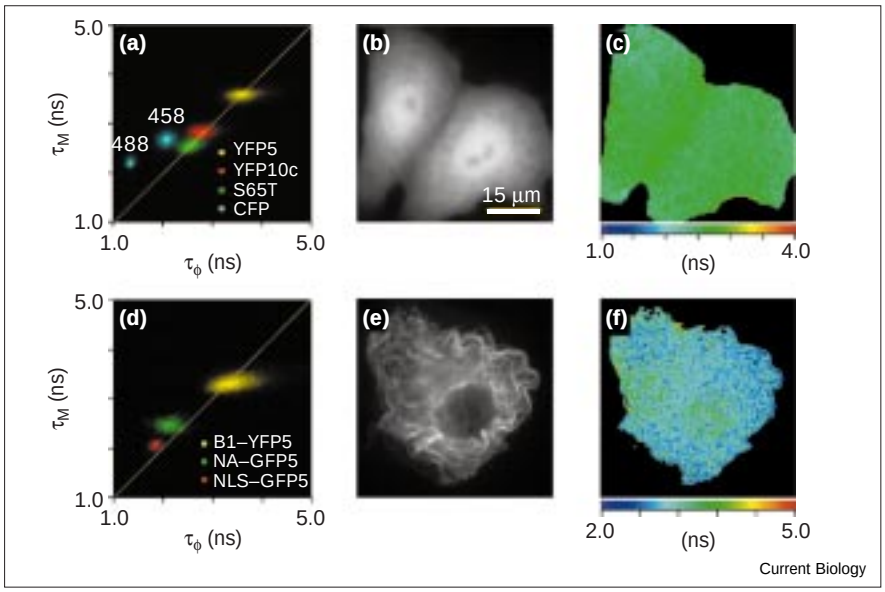

Characterisation of fluorescence lifetime properties of GFP variants by FLIM. **(a)** Two-dimensional histogram of fluorescence lifetimes determined by phase shift (τ_ϕ) and demodulation (τ_M) of four GFPs expressed in Vero cells. The CFP lifetime distributions were obtained for excitation at ~458 nm or 488 nm. **(b)** Fluorescence intensity distribution of the S65T mutant expressed in Vero cells. **(c)** Fluorescence lifetime map of the S65T mutant. The fluorescence lifetime image was calculated from the average of the phase and modulation lifetime maps. **(d)** Two-dimensional histogram of fluorescence lifetimes determined by phase shift and demodulation of B1–YFP5, NA–GFP5 and NLS–GFP5 fusion proteins. **(e)** Fluorescence intensity distribution of B1–YFP5 in Vero cells. **(f)** Fluorescence lifetime map of B1–YFP5.

brefeldin A [19]. The ability to distinguish fusion proteins labelled with different GFP variants opens up the possibility of multi-labelling imaging experiments in live cells. For this, the fluorescent fusion proteins need to retain distinct lifetimes as observed for the GFP variants alone. This was tested for several GFP fusion proteins that target specific cellular compartments (Table 2). A reduction in fluorescence lifetime seems to be a general effect of fusing GFP to other proteins (Figure 1d and Table 2). Only one of the seven GFP fusion proteins tested, B1–YFP5, exhibited a localisation-dependent lifetime — a shift from approximately 3.7 ns to 3.2 ns was observed when comparing cytosolic to microtubule-bound B1–YFP5 (Figure 1e,f) [20]. A binding-induced change in the conformational dynamics of protein residues around the YFP5 chromophore, affecting its excited state depopulation, may offer one possible explanation of this effect and could be exploited to calculate the variable fraction of microtubule-bound cyclin B1. Nevertheless, the results shown in Table 2 demonstrate a distinction between fusion proteins (for example, Figure 1d) that is sufficient for their use in multi-labelling experiments using FLIM. This was demonstrated by the determination of individual fluorescence intensity maps (Figure 2c,d,g,h,k,l,o,p) corresponding to the cellular distribution of each of two co-expressed GFP proteins using lifetime images (Figure 2b,f,j,n) and dispersion relationships (Supplementary material). The Golgi-resident enzyme NA–GFP5, in particular, is seen to localise primarily to that organelle, with some staining of reticular structures in the cytoplasm (Figure 2c), most likely corresponding to the ER. A similar distribution was frequently observed in cells expressing NA–GFP5 alone (data not shown). In contrast, the co-expressed YFP5 was distributed throughout the cell (Figure 2d). Furthermore, comparison of Figure 2d,h with Figure 2l shows that the increase in size from the fusion of YFP to cyclin B1 resulted in its exclusion from the nucleus. In Figure 2g,k,o, dominant nuclear staining is observed for GFP5 fused to a nuclear localisation signal (NLS–GFP5). Finally, the cell-surface display chimera Igκ–YFP5–PDGFR (Figure 2p) is seen to have localised to the ER and accumulated in the

Table 2

Phase and modulation lifetimes of GFP fusion proteins measured by FLIM in live cells at 37°C.

GFP fusion protein	Lifetime (ns)		Number of measurements
	τ_ϕ	τ_M	
NLS–CFP (458 nm)	2.18 ± 0.05	2.74 ± 0.04	8
NLS–CFP (488 nm)	1.35 ± 0.03	2.07 ± 0.03	3
ErbB1–EGFP*	2.11 ± 0.06	2.43 ± 0.05	7
EGFP–p110α†	2.13 ± 0.05	2.44 ± 0.04	6
NLS–GFP5	1.92 ± 0.06	2.25 ± 0.05	4
NA–GFP5 (Golgi)	2.05 ± 0.10	2.40 ± 0.05	6
NA–GFP5 (ER)	2.25 ± 0.13	2.58 ± 0.07	3
Igκ–YFP5–PDGFR	3.35 ± 0.14	3.49 ± 0.07	5
B1–YFP5	3.26 ± 0.10	3.34 ± 0.05	4

Abbreviations: NLS, nuclear localisation signal; ErbB1, epidermal growth factor receptor; p110α, catalytic subunit of phosphatidylinositol 3-kinase; NA, N-acetylglucosaminyltransferase I; Igκ, immunoglobulin κ; PDGFR, platelet-derived growth factor receptor; B1, cyclin B1. *F.S. Wouters and P.I.H.B., unpublished data. †A. de Roos and P.I.H.B., unpublished data.

Figure 2

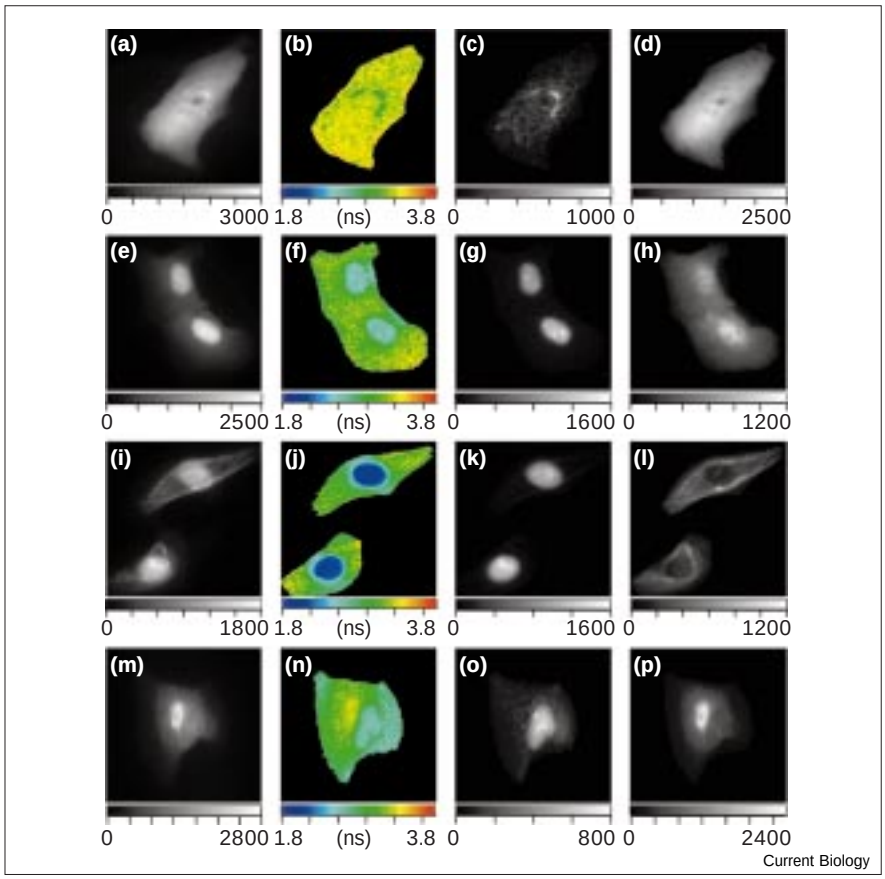

Intracellular distributions of two co-expressed GFP variants calculated from average fluorescence lifetime maps. The following proteins were co-expressed in Vero cells: **(a–d)** NA–GFP5 and YFP5; **(e–h)** NLS–GFP5 and YFP5; **(i–l)** NLS–GFP5 and B1–YFP5; and **(m–p)** NLS–GFP5 and Igκ–YFP5–PDGFR. Panels (a,e,i,m) show the total fluorescence intensity distributions, and panels (b,f,j,n) show the respective average fluorescence lifetime maps. The calculated intensity distributions of the individual proteins are shown: (c) NA–GFP5 and (d) YFP5; (g) NLS–GFP5 and (h) YFP5; (k) NLS–GFP5 and (l) B1–YFP5; and (o) NLS–GFP5 and (p) Igκ–YFP5–PDGFR.

Golgi from where it is transported to the plasma membrane and exposed to the extracellular environment. These results clearly demonstrate that FLIM offers an effective approach for disentangling the cellular distributions of two co-expressed GFP variants.

The measurement of FLIM data at a single modulation frequency sets an upper limit of three to the number of fluorescent probe distributions that can be simultaneously resolved using the dispersion relationships (Supplementary material). These were applied to lifetime maps (Figure 3b,c) for resolving the populations of co-expressed NLS–CFP, NA–GFP5 and B1–YFP5. As seen from the calculated intensity maps (Figure 3f), NLS–CFP made a relatively low contribution to the overall fluorescence (Figure 3a). The relative amount of noise seen in this image can be attributed to this fact and also to CFP fluorescent species lifetime inhomogeneity. The contributions to the total fluorescence from each of the GFP proteins were separated, however, and distributed predominantly within their expected cellular structures.

In summary, it has been shown that FLIM at a single modulation frequency can be used to image and follow the cellular distribution of two and ultimately three GFPs simultaneously. FLIM has several advantages over the use of spectral discrimination of GFP variants. The readout of data is simultaneous and requires only a single dichroic and long pass emission filter, thus collecting the majority of the emitted fluorescence. The resultant increase in detection sensitivity allows physiological amounts of GFPs to be imaged with lower light dose, thus reducing photochemical damage to cells. Furthermore, the efficient discrimination and quantification of spectrally similar GFP variants is now possible in live cells.

Materials and methods

Live cell preparation

Vero cells were plated on Matek petri dishes (Matek Corporation) in MEM supplemented with 5% foetal calf serum. Cells were microinjected with purified GFP proteins previously expressed in *Escherichia coli*, or microinjected in the nucleus with their cDNA-encoding plasmids. Dishes of cells were washed and submerged in CO_2-independent medium (GibcoBRL) before FLIM measurements at 37°C.

GFP variants and fusion constructs

YFP5 was derived from GFP5 by introducing S72A and T203Y mutations. GFP5 was derived from MmGFP [21] and differs in having a S2G mutation and the addition of serine and phenylalanine at the carboxyl terminus. A Golgi-resident enzyme consisting of GFP5 fused to

Figure 3

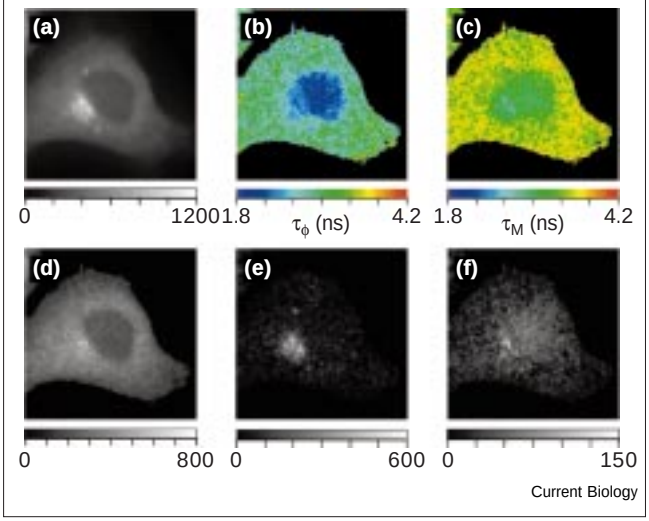

Intracellular distribution of three co-expressed GFP variants (NLS–CFP, NA–GFP5 and B1–YFP5) in Vero cells calculated from: (a) total fluorescence intensity, (b) phase and (c) modulation lifetime maps. These three images were used to calculate the intensity distributions of (d) B1–YFP, (e) NA–GFP5 and (f) NLS–CFP.

the luminal domain on N-acetylglucosaminyltransferase I (NA–GFP5) was kindly provided by D. Shima, ICRF [3]. The nuclear targetted chimeras NLS–GFP5 (kindly provided by Michael Brandeis, University of Jerusalem) and NLS–CFP were constructed by fusing the coding sequence of GFP5/CFP with the coding sequence of the nuclear bipartite nucleoplasmin localisation signal sequence (KRPAATKK-AGQAKKKK). Cyclin B1 was fused to the amino terminus of YFP5 to generate B1–YFP5. (See Supplementary material for details.) YFP5 was subcloned in the pDisplay vector (Invitrogen) to generate the cell-surface-displayed Igκ–YFP5–PDGFR.

FLIM measurement

A full description of the fluorescence lifetime imaging microscope can be found elsewhere [16]. GFPs were excited with the 488 nm argon/krypton laser line. CFPs were also excited at 457.9 nm. The detection filter block contained a dichroic beamsplitter 505LP in combination with a High Q bandpass emission filter Q535/50 BP (Chroma Technology Corporation). A Zeiss FLUAR 100 × /1.3 NA DIC oil objective and a LD Achroplan 40 × /0.6 NA Corr Ph2 air objective were used for live cell and pH titration experiments, respectively. FLIM data were recorded at either 80.218 MHz or 80.244 MHz. Details of the numerical methods can be found in the Supplementary material.

Supplementary material

Additional methodological details and a figure showing the pH dependence of GFP lifetimes are published with this article on the internet.

Acknowledgements

We thank T. Hunt (ICRF) for generous support and G. Warren for critical evaluation of the manuscript.

References

1. Rizzuto R, Brini M, Degiorgi F, Rossi R, Heim R, Tsien RY, *et al.*: Double-ing of subcellular structures with organelle-targeted GFP mutants ***in vivo***. *Curr Biol* 1996, 6:183-188.
2. ZernickaGoetz M, Pines J, Ryan K, Siemering KR, Haseloff J, Evans MJ, *et al.*: An indelible lineage marker for Xenopus using a mutated green fluorescent protein. *Development* 1996, 122:3719-3724.
3. Shima DT, Haldar K, Pepperkok R, Watson R, Warren G: Partitioning of the Golgi apparatus during mitosis in living HeLa cells. *J Cell Biol* 1997, 137:1211-1228.
4. Girotti M, Banting G: TGN38-green fluorescent protein hybrid proteins expressed in stably transfected eukaryotic cells provide a tool for the real-time, in vivo study of membrane traffic pathways and suggest a possible role for ratTGN38. *J Cell Sci* 1996, 109:2915-2926.
5. Oancea E, Teruel MN, Quest AFG, Meyer T: Green fluorescent protein (GFP)-tagged cysteine-rich domains from protein kinase C as fluorescent indicators for diacylglycerol signaling in living cells. *J Cell Biol* 1998, 140:485-498.
6. Ellenberg J, Lippincott-Schwartz J, Presley JF: Two color green fluorescent protein time-lapse imaging. *Biotechniques* 1998, 25:838-946.
7. Heim R, Cubitt AB, Tsien RY: Improved green fluorescence. *Nature* 1995, 373:663-664.
8. Cormack BP, Valdivia RH, Falkow S: FACS-optimized mutants of the green fluorescent protein (GFP). *Gene* 1996, 173:33-38.
9. Heim R, Tsien RY: Engineering green fluorescent protein for improved brightness, longer wavelengths and fluorescence resonance energy-transfer. *Curr Biol* 1996, 6:178-182.
10. Tsien RY: The green fluorescent protein. *Annu Rev Biochem* 1998, 76:509-538.
11. So PTC, French T, Yu WN, Berland K, Dong CY, Gratton E: Time-resolved fluorescence microscopy using two-photon excitation. *Bioimaging* 1995, 3:1-15.
12. Carlsson K, Liljeborg A: Confocal fluorescence microscopy using spectral and lifetime information to simultaneously record four fluorophores with high channel separation. *J Microsc* 1997, 185:37-46.
13. Lakowicz JR, Berndt K: Lifetime-selective fluorescence imaging using an rf phase-sensitive camera. *Rev Sci Instrum* 1991, 62:1727-1734.
14. Gadella TWJ Jr, Jovin TM, Clegg RM: Fluorescence lifetime imaging microscopy (FLIM) - spatial resolution of microstructures on the nanosecond time-scale. *Biophys Chem* 1993, 48:221-239.
15. Schneider PC, Clegg RM: Rapid acquisition, analysis, and display of fluorescence lifetime-resolved images for real-time applications. *Rev Sci Instrum* 1997, 68:4107-4119.
16. Squire A, Bastiaens PIH: Three dimensional image restoration in fluorescence lifetime imaging microscopy. *J Microsc* 1999, 193:36-49.
17. Kneen M, Farinas J, Li YX, Verkman AS: Green fluorescent protein as a noninvasive intracellular pH indicator. *Biophys J* 1998, 74:1591-1599.
18. Llopis J, McCaffery JM, Miyawaki A, Farquhar MG, Tsien RY: Measurement of cytosolic, mitochondrial, and Golgi pH in single living cells with green fluorescent proteins. *Proc Natl Acad Sci USA* 1998, 95:6803-6808.
19. Scheel J, Pepperkok R, Lowe M, Griffiths G, Kreis TE: Dissociation of coatomer from membranes is required for brefeldin A-induced transfer of Golgi enzymes to the endoplasmic reticulum. *J Cell Biol* 1997, 137:319-333.
20. Jackman M, Firth M, Pines J: Human cyclins B1 and B2 are localized to strikingly different structures - B1 to microtubules, B2 primarily to the Golgi-apparatus. *EMBO J* 1995, 14:1646-1654.
21. ZernickaGoetz M, Pines J, Hunter SM, Dixon JPC, Siemering KR, Haseloff J, *et al.*: Following cell fate in the living mouse embryo. *Development* 1997, 124:1133-1137.
22. Miyawaki A, Llopis J, Heim R, McCaffery JM, Adams JA, Ikura M, *et al.*: Fluorescent indicators for Ca^{2+} based on green fluorescent proteins and calmodulin. *Nature* 1997, 388:882-887.

Supplementary material

Simultaneous detection of multiple green fluorescent proteins in live cells by fluorescence lifetime imaging microscopy

Rainer Pepperkok, Anthony Squire, Stephan Geley and Philippe I.H. Bastiaens

Current Biology 1 March 1999, 9:269–272

Supplementary materials and methods

Construction of YFP5

MmGFP5 [S1] was amplified from pCMX-GFP5 (kindly provided by J. Pines) in two fragments using primer pair ATGCGGCCGCGAATTC-GCCACCATGGGTAAAGGAGAAGAACTT and CAAGTGTTGGCC-AGGGAACAG and primer pair AAGGATCCTCTAGAAGCTTTTGTA TAGTTCATCCATG and CTGTTCCCTGGCCAACACTTG using *Pfu* polymerase (Stratagene) to destroy the internal *Nco*I restriction site (underlined) by a silent point mutation in Pro56 (cca→ccc). In addition, a Kozak translational consensus sequence (GCCACCATGG) was introduced, thereby creating an amino-terminal *Nco*I site and changing the second amino acid from serine to glycine. The carboxyl terminus contains a *Hind*III site in the open reading frame and thus adds a serine and phenylalanine at the carboxyl terminus. This GFP variant does not have altered residues involved in the fluorescent properties and is called GFP5 to distinguish it from MmGFP5. The PCR product was subcloned as a *Not*I/*Bam*HI as well as an *Eco*RI/*Xba*I fragment into pBluescript KS(–) (Stratagene) generating pSK-GFP5 and pSK-GFP5II, respectively. The *Eco*RI/*Xba*I fragment was also subcloned into the mammalian expression vector pEFT7MCS. This vector is based on pEF-BOS [S2]. A modified version of pEF-BOS containing a Neo resistance expression cassette, pEF1-Neo, was kindly provided by G. Baier, University of Innsbruck. The Neo resistance expression cassette was deleted to make the vector smaller and a T7 RNA polymerase promoter site as well as several unique restriction enzyme sites were introduced downstream of the human EF1α promoter and the SV40 polyadenylation site. The red-shifted mutant YFP5 was generated by PCR-mediated site-directed mutagenesis of GFP5. The mutations S72A and T203Y were introduced in GFP5 by using the following primer pairs: ATGCGGCCGCGAATTCGCCACCATGGGTAAAGGAGAAGAACTT and CTGGGTATCTTGCGAAGCATTGTACGTACAATGCTTCGCAA-GATACCCAG, and GAAAGGGCAGATTGATAGGACAGGTAATG-CATTACCTGTCCTATCAATCTGCCCTTTC and AAGGATCCTCTA GAAGCTTTTGTATAGTTCATCCATG, where underlined nucleotides indicate mismatches. The final PCR product was gel-purified, digested with *Eco*RI and *Xba*I and subcloned into pEFT7MCS. The introduced mutations were verified by sequencing using sequenase.

GFP fusion constructs

The construction of NA–GFP5 (kindly provided by D. Shima, ICRF) is described elsewhere [S3]. NLS–GFP5 (kindly provided by Michael Brandeis, University of Jerusalem) was constructed by subcloning an *Nco*I/*Xba*I fragment of GFP5 containing the entire open reading frame into pEFplink2. An oligonucleotide encoding the nucleoplasmin bipartite NLS sequence (KRPAATKKAGQAKKKK) was inserted into the *Nco*I site (pEFplink2-NLS–GFP5). For the construction of NLS–CFP, ECFP was amplified from pRSETb-ECFP (kindly provided by Roger Tsien, University of California) and an *Nco*I/*Xba*I fragment was subcloned into the *Nco*I/*Xba*I sites of pEFplink2-NLS–GFP5 thus exchanging the GFP for the CFP. Cyclin B1 was fused to the amino terminus of YFP5 by subcloning a *Nco*I/*Xba*I fragment of YFP5 into pEFplink2 to get pEF-plink2-YFP5. An *Nco*I fragment containing the cyclin B1 open reading frame was excised from pEFplink2-B1–GFP5 (kindly provided by M. Brandeis, University of Jerusalem) and inserted into the *Nco*I site of pEFplink2-YFP5. Cell-surface-displayed Igκ–YFP5–PDGFR was constructed from cDNA amplified from pEFT7MCS-YFP5 using primers TAGATAGATCTGGTAAAGGAGAAGAACTTTTCACTGG and TAG-TAGTCGACGCTTTTGTATAGTTCATCCATGCCATG. The PCR product was gel purified, digested with restriction enzymes *Bgl*II and *Sal*I and subcloned into the *Bgl*II/*Sal*I cut plasmid pDisplay (Invitrogen).

pH dependence of the lifetime of recombinant GFPs in vitro

Between 1 mg/ml and 4 mg/ml of the mutant GFP proteins S65T, YFP10c, and CFP were diluted up to 50-fold in 20 mM Hepes or 0.1 M Tris at a pH of 3.9, 5.4, 6.9, 7.3 and 8.8. Sample dishes for each mutant GFP in turn were prepared by pipetting a pH titration series of 2.5 μl drops onto the coverslip region of a Matek petri dish just prior to FLIM measurements at room temperature (see Figure S1).

FLIM setup

A full description of the fluorescence lifetime imaging microscope can be found elsewhere [S4]. In brief, a scientific grade charge-coupled device (CCD) camera (Photometrics Quantix), microchannel plate image intensifier (Hammamatsu C5825), standing wave acousto-optic modulators (Intra-Action Corporation, Belwood) and an Argon/Krypton mixed gas laser (Coherent Innova 70C) configured around an inverted microscope (Zeiss Axiovert 135 TV) constitute the heart of the instrument, which operates as a phase- and modulation-sensitive imaging fluorimeter. The acousto-optic modulators driven by the amplified output of a high frequency signal generator (Marconi 2023) provide a means of modulating the laser illumination source. Homodyne phase-sensitive detection of the resulting sample fluorescence emission is achieved by modulation of the gain characteristics of the image intensifier, placed at the TV port of the microscope, using a second signal generator phase locked to the first. The CCD camera records a series of phase-sensitive images at the phosphor screen output of the image intensifier which are stored on a Unix Workstation (Silicon Graphics O_2) and Fourier transform routines written for the image processing package SCIL-Image (version 1.3, TNO Institute of Applied Physics) were used to determine both the phase- and modulation-dependent fluorescence lifetimes. The microscope was enclosed in a temperature-stabilised incubator to enable live cell experiments at 37°C.

Numerical methods

A full mathematical description of fluorescence lifetime fluorimetry is given elsewhere [S4–S6]. Recapping in brief, and considering single frequency f only: exciting a fluorescence sample with a sinusoidal source of excitation $E(t)$ results in sinusoidally modulated fluorescence emission $F(t)$ that is both phase-shifted and demodulated relative to the excitation source. The excitation $E(t)$ and fluorescence emission $F(t)$ (in arbitrary units) are given by:

$$E(t) = E_0(1 + M_E Cos(\omega t + \Theta)) \quad (1)$$

$$F(t) = F_0(1 + M_F Cos(\omega t + \Theta')) \quad (2)$$

where $\omega = 2\pi f$ is the circular frequency of oscillation, E_0 and F_0 are the respective time invariant (DC) components of the modulations, M_E and M_F are the relative modulation amplitudes of the time variant (AC) part of the oscillations; and Θ and Θ' are the respective phases relative to some arbitrary electronic phase setting. Thus, the phase lag $\Delta\phi$ and demodulation M of the fluorescence emission are defined by:

$$\Delta\phi = \Theta - \Theta' \quad (3)$$

$$M = M_F/M_E \quad (4)$$

The application of Fourier routines to phase-dependent sample images, collected using FLIM, gives the DC, AC sine and AC cosine components of the signal at every pixel. From these components, the phase lag and demodulation are calculated, both of which are related to the

Figure S1

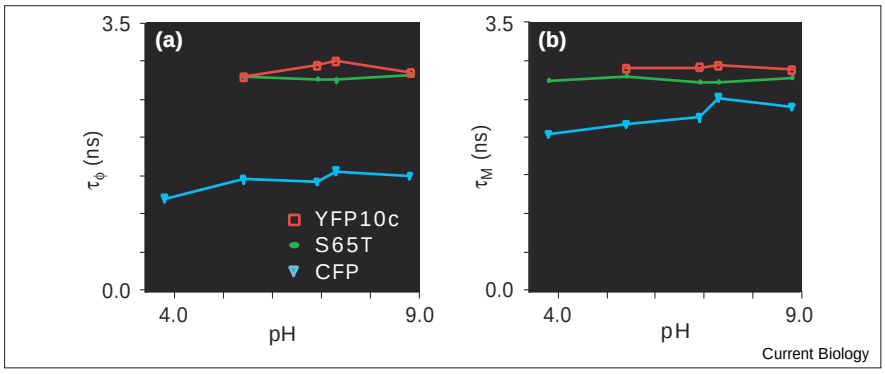

The figure shows the pH dependence of the (a) phase and (b) modulation lifetimes of the three GFP mutants measured (YFP10c, S65T and CFP). Each point on the graph is the average of two independent experiments.

distributions of fluorescence lifetimes and relative amounts of distinct fluorophores within the sample through the dispersion relationships:

$$MSin(\Delta\phi) = \sum_{j=1}^{N}\left(\frac{\omega\alpha_j\tau_j}{1+\omega^2\tau_j^2}\right) \quad (5a)$$

$$MCos(\Delta\phi) = \sum_{j=1}^{N}\left(\frac{\alpha_j}{1+\omega^2\tau_j^2}\right) \quad (5b)$$

Here, α_j is the fractional contribution to the total fluorescence from the jth emitting species with fluorescence lifetime τ_j, thus:

$$\sum_{j=1}^{N}\alpha_j = 1 \quad (6)$$

where α_j is related to the fractional decay amplitude a_j by:

$$\alpha_j = a_j\tau_j \quad (7)$$

Images of the phase and modulation lifetimes at excitation frequency ω are generated using the relationships:

$$\tau_\phi = \frac{1}{\omega}Tan(\Delta\phi) \quad (8a)$$

$$\tau_M = \frac{1}{\omega}\sqrt{\frac{1}{M^2}-1} \quad (8b)$$

For FLIM data measured at a single frequency, Equations 5 and 6 can be used to determine a maximum of three unknown parameters.

For samples consisting of a mixture of two fluorophore species in which the individual fluorescence lifetimes τ_1 and τ_2 of both fluorophore species are known, the sum of Equations 5 and 6 can be solved for α_1:

$$\alpha_1 = \frac{\left(1+\tau_1^2\omega^2\right)\left(1-\omega\tau_2-\psi\left(1+\omega^2\tau_2^2\right)\right)}{\omega(\tau_1-\tau_2)\left(\omega(\tau_1+\tau_2+\omega\tau_2)-1\right)} \quad (9a)$$

where

$$\psi = \frac{1+\omega\tau_\phi}{\sqrt{1+\omega^2\tau_M^2}\sqrt{1+\omega^2\tau_\phi^2}} \quad (9b)$$

The fluorescence intensity from the fluorophore corresponding to α_1 is obtained by multiplying the α_1 and DC images. The same procedure is applied to α_2, calculated from the trivial relationship $\alpha_2 = 1-\alpha_1$.

For samples composed of a mixture of three fluorophore species, Equations 5 and 6 are solved for the α_js with N = 3 giving:

$$\alpha_1 = \frac{1+\tau_1^2\omega^2}{(\tau_1-\tau_2)(\tau_1-\tau_3)}\left(\left(1-M+M\omega^2\tau_2\tau_3\right)Cos(\phi)-M\omega(\tau_2+\tau_3)Sin(\phi)\right) \quad (10a)$$

$$\alpha_2 = -\frac{1+\tau_2^2\omega^2}{(\tau_1-\tau_2)(\tau_2-\tau_3)}\left(\left(1-M+M\omega^2\tau_1\tau_3\right)Cos(\phi)-M\omega(\tau_1+\tau_3)Sin(\phi)\right) \quad (10b)$$

$$\alpha_3 = \frac{1+\tau_3^2\omega^2}{(\tau_1-\tau_3)(\tau_2-\tau_3)}\left(\left(1-M+M\omega^2\tau_1\tau_2\right)Cos(\phi)-M\omega(\tau_1+\tau_2)Sin(\phi)\right) \quad (10c)$$

As above, multiplying the α_j and DC images gives the fluorescence intensity contribution from the jth species to the DC image.

References

S1. ZernickaGoetz M, Pines J, Hunter SM, Dixon JPC, Siemering KR, Haseloff J, *et al.*: Following cell fate in the living mouse embryo. *Development* 1997, 124:1133-1137.

S2. Mizushima S, Nagata S: pEF-BOS a powerful mammalian expression vector. *Nucleic Acids Res* 1990, 18:5322.

S3. Shima DT, Haldar K, Pepperkok R, Watson R, Warren G: Partitioning of the Golgi apparatus during mitosis in living HeLa cells. *J Cell Biol* 1997, 137:1211-1228.

S4. Squire A, Bastiaens PIH: Three dimensional image restoration in fluorescence lifetime imaging microscopy. *J Microsc* 1999, 193:36-49.

S5. Weber G: Resolution of the fluorescence lifetimes in a heterogeneous system by phase and modulation measurements. *J Phys Chem* 1981, 85:949-953.

S6. Clegg RM, Schneider PC: Fluorescence lifetime-resolved imaging microscopy: a general description of lifetime-resolved imaging measurements. In *Fluorescence Microscopy and Fluorescence Probes.* Edited by Slavik J. New York: Plenum Press; 1996:15-33.